

Magnetic Properties of a Manganese(II) Trinuclear Complex Involving a Tridentate Schiff-Base Ligand

Radovan Herchel,^{*,†} Roman Boča,^{†,‡} Milan Gembický,^{‡,§} Karsten Falk,^{||} Hartmut Fuess,^{||} Wolfgang Haase,^{||} and Ingrid Svoboda^{||}

Department of Chemistry, University of SS. Cyril and Methodius, SK-917 01 Trnava, Slovakia,
Department of Inorganic Chemistry, Slovak Technical University, SK-812 37 Bratislava, Slovakia,
Department of Chemistry, State University of New York at Buffalo, Buffalo,
New York 14260-3000, and Eduard-Zintl-Institute of Inorganic and Physical Chemistry,
Materials Science, Darmstadt University of Technology, D-64287 Darmstadt, Germany

Received September 11, 2006

The Schiff condensation of 2-pyridinecarboxaldehyde *N*-oxide with 2-aminophenol gave a tridentate ligand, abbreviated as Hpozap. This ligand bears the functionality of a terminating group in a trinuclear complex $[\text{Mn}(\text{pozap})\text{Mn}(\text{ac})_4\text{Mn}(\text{pozap})]$, where ac^- is the acetate bridge. The magnetic data were treated simultaneously during the fitting procedure with the spin Hamiltonian containing isotropic exchange, the zero-field splitting parameters, and the molecular-field correction and resulted in $J_{\text{Mn}-\text{Mn}}/hc = -4.73 \text{ cm}^{-1}$, $g_{\text{Mn}(t)} = 1.96$, $D_{\text{Mn}(t)}/hc = -0.45 \text{ cm}^{-1}$, and $zJ/hc = +0.45 \text{ cm}^{-1}$ with ground state $S = 5/2$, where $t =$ terminal atom. At low temperature, the features of a ferromagnetic correlation become evident.

The pyridine *N*-oxide analogues of the Schiff-base complexes have been widely studied in the past decade. 2-Pyridinecarboxaldehyde *N*-oxide (poxal) serves as a precursor for several Schiff-type condensations with aliphatic and/or aromatic amines yielding bidentate, tridentate, tetradentate, pentadentate, and hexadentate ligands. Our key tridentate ligand (Hpozap) can be prepared by the condensation reaction $\text{poxal} + 2\text{-NH}_2\text{PhOH} \rightarrow \text{Hpozap}$.

Mononuclear complexes of the type $[\text{M}^{\text{II}}(\text{pozap})^{-1}\text{A}^{-1}] \cdot \text{sol}$ with a coligand $\text{A} = \text{NO}_3^-$ or ac^- have been reported.¹ The structure of the trinuclear $[\text{Zn}(\text{pozap})\text{Zn}(\text{ac})_4\text{Zn}(\text{pozap})]$ complex was determined (two polymorphs), and the magnetic properties of the trinuclear complex $[\text{Cu}_3(\text{pozap})_2\text{Cl}_4]$ were studied.²

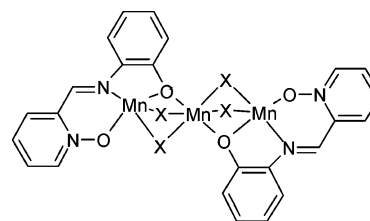


Figure 1. Sketch of the trinuclear complex **1** ($\text{X} = \text{ac}^-$).

The present communication deals with a trinuclear Mn(II) complex $[\text{Mn}_3(\text{ac})_4(\text{pozap})_2]$ (**1**) and its magnetic properties. Et_3N ($V_1 = 0.2 \text{ cm}^3$) was added to a cold solution of Hpozap ($n_1 = 1.0 \text{ mmol}$) in acetonitrile ($V_2 = 15 \text{ cm}^3$) and methanol ($V_3 = 40 \text{ cm}^3$). This mixture was combined with a solution of $\text{Mn}(\text{OAc})_2 \cdot 4\text{H}_2\text{O}$ ($n_2 = 1.0 \text{ mmol}$) in methanol ($V_4 = 20 \text{ cm}^3$), and the system was left to crystallize. After 24 h, small brown crystals were separated on the fritta funnel. Yield: 0.14 g. Anal. Calcd for $\text{C}_{32}\text{H}_{30}\text{N}_4\text{O}_{12}\text{Mn}_3$ ($M_r = 827.42$): C, 46.4; H, 3.65; N, 6.77; Mn, 19.9. Found: C, 46.9; H, 3.85; N, 6.91; Mn, 19.7.

The expected structural motif of the complex is shown in Figure 1. It is an analogue of the trinuclear Zn(II) complex whose structure has been reported.² The IR spectra of **1** are similar to those of the Zn(II) analogues; X-ray powder diffraction patterns show that the structure of **1** closely resembles that of $\alpha\text{-}[\text{Zn}_3(\text{ac})_4(\text{pozap})_2] \cdot \text{H}_2\text{O}$ (see Figures S1 and S2 in the Supporting Information).

The temperature dependence of the magnetization at $B = 0.1, 2.0,$ and 5.0 T (transformed to the mean magnetic susceptibility) has been recorded with a SQUID apparatus (Quantum Design). A correction of the underlying diamagnetism was estimated on the basis of Pascal constants as $\chi_{\text{dia}} = -4.3 \times 10^{-9} \text{ m}^3 \text{ mol}^{-1}$.³ The effective magnetic moment is calculated in SI units as $\mu_{\text{eff}}/\mu_B = 798[(\chi_{\text{mol}} - \chi_{\text{dia}})T]^{1/2}$.

Magnetization measurements up to $B = 5.5 \text{ T}$ at different temperatures and alternating current susceptibility measure-

* To whom correspondence should be addressed. E-mail: radovan.herchel@ucm.sk. Fax: +421 33 557 3360.

[†] University of SS. Cyril and Methodius.

[‡] Slovak Technical University.

[§] State University of New York at Buffalo.

^{||} Darmstadt University of Technology.

(1) Baran, P.; Elias, H.; Svoboda, I.; Wltschek, G. In *Current Trends in Coordination Chemistry*; Ondrejovič, G., Sirota, A., Eds.; STU University Press: Bratislava, Slovakia, 1995; p 309.

(2) Gembický, M.; Baran, P.; Boča, R.; Fuess, H.; Svoboda, I.; Valko, M. *Inorg. Chim. Acta* **2000**, *303*, 75.

(3) König, E. *Landolt-Börnstein*; Springer: Berlin, 1966; Neue Serie Vol. 2, pp 1–16.

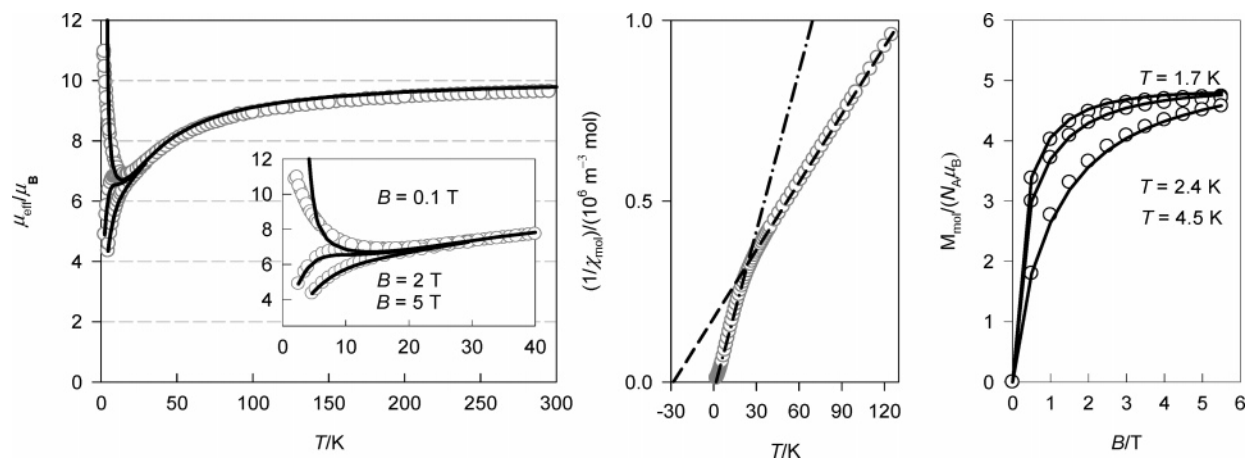


Figure 2. Magnetic functions for **1**. Left: temperature dependence of the effective magnetic moment (calculated from the temperature dependence of magnetization at $B = 0.1, 2.0,$ and 5.0 T). Center: inverse susceptibility at $B = 0.1$ T and its extrapolation. Right: field dependence of magnetization at $T = 1.7, 2.4,$ and 4.5 K. Empty circles: experimental points. Full line: fitted data.

ments at different frequencies have been done with an alternating current susceptometer/magnetometer (LakeShore, model 7225).

The experimental magnetic functions are shown in Figure 2. The magnetic susceptibility monotonously increases upon cooling from $T = 300$ to 4.2 K. The effective magnetic moment at $T = 300$ K adopts the value of $\mu_{\text{eff}} = 9.6 \mu_{\text{B}}$. For a low applied field ($B = 0.1$ T), the effective magnetic moment rises rapidly, and at $T = 2.0$ K, it adopts a value of $\mu_{\text{eff}} = 10.8 \mu_{\text{B}}$.

The inverse susceptibility ($1/\chi_{\text{mol}}$) vs T is linear in the higher-temperature (HT) range $T = 30\text{--}300$ K and can be fitted to the Curie–Weiss law $\chi_{\text{mol}} = N_{\text{A}}\mu_0\mu_{\text{eff}}^2/[3k(T - \Theta)]$, resulting in a negative Weiss constant $\Theta_{\text{HT}} = -29$ K and $\mu_{\text{eff}} = 10.0 \mu_{\text{B}}$, which is in agreement with $\mu_{\text{eff}} = 9.6 \mu_{\text{B}}$ at 300 K. This indicates a dominant antiferromagnetic coupling that operates above $T > 30$ K. Upon further cooling, the slope of this function is altered, and below $T < 17$ K, it becomes again nearly linear with $\Theta_{\text{LT}} = +1.9$ K and $\mu_{\text{eff}} = 6.4 \mu_{\text{B}}$, which is the expected value for the ground state $S = 5/2$. This unusual behavior is reproducible: it was found for three samples prepared independently. It seems that below $T < 17$ K a ferromagnetic correlation applies.

The ground state $S = 5/2$ has been confirmed by the measurement of the magnetization until $B = 5.5$ T at low temperatures (Figure 2). The theoretical value of the magnetization per complex for $g = 2.0$ is $M_{\text{mol}}/N_{\text{A}}\mu_{\text{B}} = 5.0$ when $S = 5/2$, and this is approached at $T = 4.5$ K and more rapidly at lower temperatures of $T = 2.4$ and 1.7 K.

To a first approximation, the higher-temperature window of the magnetic data has been successfully fitted with the spin Hamiltonian that accounts for the isotropic exchange of adjacent centers and the Zeeman term.⁴ The continuation of the “theoretical” curve below 35 K would lead to a plateau with $\mu_{\text{eff}}/\mu_{\text{B}} = 5.55$ ($T = 2.0$ K; $B = 0.1$ T) in analogy with observations for similar systems.^{5–10} However, the situation

for **1** is different: the effective magnetic moment ($B = 0.1$ T) passes through a minimum at $T = 17$ K and then rapidly increases upon subsequent cooling down to $T = 2.0$ K.

In order to explain the observed low-temperature behavior, an additional molecular-field correction and a single-ion zero-field splitting (ZFS) have been considered

$$\hat{H}^{(2)}(a) = -\mathcal{J}\hbar^{-2}(\vec{S}_{\text{t1}} \cdot \vec{S}_{\text{c}} + \vec{S}_{\text{c}} \cdot \vec{S}_{\text{t2}}) + \sum_A^{\text{t1,c,t2}} \mu_{\text{B}}\hbar^{-1}B_a g_A \hat{S}_{Aa} + \sum_A^{\text{t1,t2}} D_A \hbar^{-2}[\hat{S}_{Az} \cdot \hat{S}_{Az} - (\vec{S}_A \cdot \vec{S}_A)/3] - (z_j)\hbar^{-1}\langle S_a \rangle_T \hat{S}_a \quad (1)$$

where z_j is a common molecular-field parameter, $\langle S_a \rangle_T$ is a thermal average of the spin, and D_A is the ZFS parameter. Because the terminal Mn(II) centers are only pentacoordinated $\{\text{MnN}_2\text{O}_3\}$, this predisposes the ZFS parameters $D_{\text{t1}} = D_{\text{t2}} \neq 0$. The central Mn(II) unit possesses a nearly octahedral coordination sphere $\{\text{MnO}_6\}$, and therefore it is expected that $D_{\text{c}} = 0$ and $g_{\text{c}} = 2.0$.¹¹

Molar magnetization was calculated through the partition function $M_a = N_{\text{A}}kT (\partial \ln Z_a/\partial B)$ for $a = x, z$ and then averaged for the powder sample as $M_{\text{av}} = (2M_x + M_z)/3$. Because the average spin in eq 1 needs eigenvectors, the equation has been solved by an iterative, time-demanding procedure.

The experimental data sets (temperature dependence of the magnetization at $B = 0.1, 2,$ and 5 T and field dependence of the magnetization at $T = 1.7, 2.4,$ and 4.5 K) were treated simultaneously during the fitting procedure; this helps in an

(4) The best-fitted parameters with an isotropic exchange model are $g_{\text{Mn}} = 1.93$ and $J_{\text{Mn–Mn}}/\hbar c = -3.51 \text{ cm}^{-1}$ (Figure S3 in the Supporting Information). These values are close to those reported for similar trinuclear Mn(II), acetate-bridged complexes, as reviewed in Table 1.

- (5) Menage, S.; Vitols, S. E.; Bergerat, P.; Codjovi, E.; Kahn, O.; Girerd, J. J.; Guillot, M.; Solans, X.; Calvet, T. *Inorg. Chem.* **1991**, *30*, 2666.
 (6) Rardin, R. L.; Poganiuch, P.; Bino, A.; Goldberg, D. P.; Tolman, W. B.; Liu, S. C.; Lippard, S. J. *J. Am. Chem. Soc.* **1992**, *114*, 5240.
 (7) Zhong, Z. J.; You, X. Z. *Polyhedron* **1994**, *13*, 2157.
 (8) Tangoulis, V.; Malamataris, D. A.; Soulti, K.; Stergiou, V.; Raptopoulou, C. P.; Terzis, A.; Kabanos, T. A.; Kessissoglou, D. P. *Inorg. Chem.* **1996**, *35*, 4974.
 (9) Reynolds, R. A.; Dunham, W. R.; Coucouvanis, D. *Inorg. Chem.* **1998**, *37*, 1232.
 (10) Adams, H.; Fenton, D. E.; Cummings, L. R.; McHugh, P. E.; Ohba, M.; Okawa, H.; Sakiyama, H.; Shiga, T. *Inorg. Chim. Acta* **2004**, *357*, 3648.
 (11) Boča, R. *Struct. Bonding* **2006**, *117*, 1.

Table 1. Magnetic Parameters of Linear Trinuclear Mn(II), Acetate-Bridged Complexes

complex	$(J_{c-}/hc)/\text{cm}^{-1}$	$(J_{t-}/hc)/\text{cm}^{-1}$	g_{Mn}	$(D_{\text{Mn}}/hc)/\text{cm}^{-1}$	$(zj/hc)/\text{cm}^{-1}$	method ^a	ref
[Mn ₃ (ac) ₆ (bpy) ₂]	-4.4		1.99			S	5
	-4.4		1.985			M	
[Mn ₃ (ac) ₆ (BIPhMe) ₂]	-5.6	-0.18	2.0		$\Theta = -0.24$ K	S	6
[Mn ₃ (ac) ₂ (bpc) ₂ (py) ₄ (H ₂ O) ₂]·0.5H ₂ O	-2.86		1.95			S	7
[Mn ₃ (ac) ₆ (pybim) ₂]	-3.8		2.02		-0.1	S	8
	-3.6		2.04			M	
[Mn ₃ (ac) ₈ (Et ₄ N) ₂]	-11.2	+1.4	2.0			S	9
[Mn ₃ (L) ₂ (ac) ₂ (NCS) ₂]·CH ₃ OH·H ₂ O	-2.0		2.0			S	10
[Mn ₃ (ac) ₄ (poxap) ₂]	-4.73		t, 1.96, c, 2.0	t, -0.45, c, 0.0	+0.45	S, M	this work

^a S = magnetic susceptibility; M = magnetization.

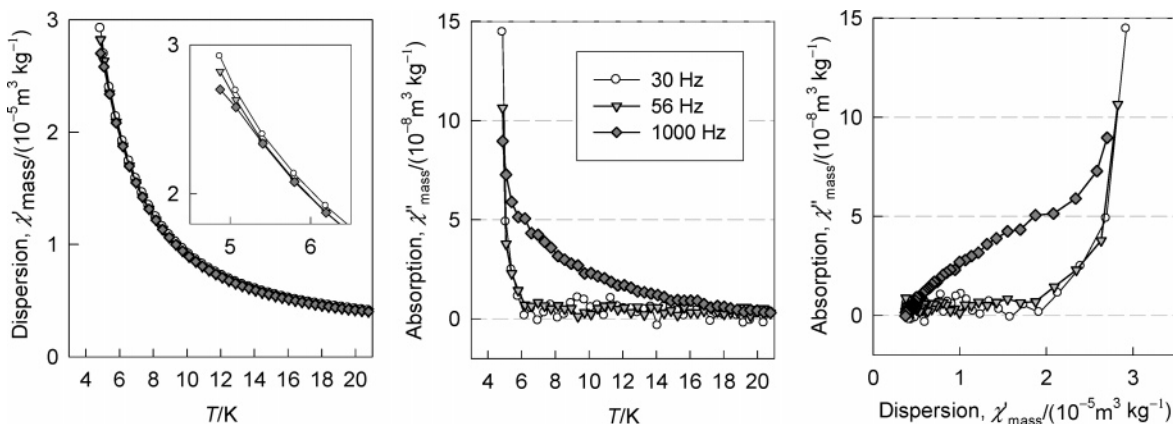


Figure 3. Alternating current (ac) susceptibility data on **1** at $f = 30, 56,$ and 1000 s^{-1} . $H_{\text{dc}} = 690 \text{ A m}^{-1}$ (9 Oe); $H_{\text{ac}} = 398 \text{ A m}^{-1}$ (5 Oe).

unambiguous determination of the magnetic parameters. The results of the fitting procedure are collected in Table 1 and displayed in Figure 2. Values of the isotropic exchange constant $J_{c-}/hc = -4.73 \text{ cm}^{-1}$ and g factor $g_{11} = g_{12} = 1.96$, for fixed $g_c = 2.0$, are in good agreement with data published so far for analogous complexes. The local anisotropy on terminal Mn(II) centers $D/hc = -0.45 \text{ cm}^{-1}$ is typical for pentacoordinated Mn(II) complexes.¹² Molecular-field correction is of a ferromagnetic nature, $zj/hc = +0.45 \text{ cm}^{-1}$, and it is substantial for a successful data fitting. It can be concluded that the prepared linear trinuclear Mn(II) complex exhibits an antiferromagnetic exchange between adjacent centers and a ferromagnetic intermolecular interaction, which is responsible for a high effective magnetic moment at $T = 2 \text{ K}$.

The magnetic parameters have been used for the reconstruction of the zero-field energy levels; these are displayed in Figure S4 in the Supporting Information. The ground state is $S = 5/2$, which is in agreement with the magnetization curves.

The magnetization measurements at $T = 1.8$ and 2.0 K were done with the field directions between $B = -1.0$ and $+1.0 \text{ T}$ in order to identify an eventual hysteresis (Figure S5 in the Supporting Information). Because the magnetization data for reversed fields are almost identical within experimental error, the existence of hysteresis is not unambiguously proven.

The alternating current susceptibility measurements in the dual mode (Figure 3) show that the out-of-phase susceptibil-

ity (absorption) starts to increase below $T < 17 \text{ K}$; it is a frequency-dependent quantity. However, it does not pass through a maximum either until $T = 4.2 \text{ K}$ or above $T = 1.8 \text{ K}$ (not shown). It can be expected that below $T < 1.8 \text{ K}$ the complex **1** could behave as a single-molecule magnet. There are predispositions for such a behavior: the ground-state $S = 5/2$, negative single-ion anisotropy of terminal Mn(II) centers, and the frequency dependence of the alternating current susceptibility. This expectation is supported also by the measurements at low static fields showing features of saturation around 1.7 K (Figure S6 in the Supporting Information). The Cole–Cole plot (absorption vs dispersion), however, does not follow the usual semicircle dependence; this indicates rather complex dynamic processes at low temperature; see also a recent report.¹³

Acknowledgment. Grant agencies and project sponsors (Slovakia, VEGA 1/2453/05, APVT 20-005204, VEGA 1/3584/06, MŠ SR-MVTS; Germany, DAAD, DFG) are acknowledged for their financial support.

Supporting Information Available: IR spectra for related systems and experimental and theoretical X-ray powder diffraction patterns (Figures S1 and S2), a fit of magnetic data for isotropic exchange spin Hamiltonian (Figure S3), a reconstruction of the zero-field energy levels (Figure S4), reverse magnetization measurements at $T = 1.8$ and 2.0 K (Figure S5), and field-cooled magnetization at low fields until $T = 1.4 \text{ K}$ (Figure S6). This material is available free of charge via the Internet at <http://pubs.acs.org>.

IC061717B

(12) Duboc, C.; Astier-Perret, V.; Chen, H. Y.; Pecaut, J.; Crabtree, R. H.; Brudvig, G. W.; Collomb, M. N. *Inorg. Chim. Acta* **2006**, *359*, 1541.

(13) Yang, E. C.; Wernsdorfer, W.; Zakharov, L. N.; Karaki, Y.; Yamaguchi, A.; Isidro, R. M.; Lu, G. D.; Wilson, S. A.; Rheingold, A. L.; Ishimoto, H.; Hendrickson, D. N. *Inorg. Chem.* **2006**, *45*, 529.